Journal of Solid State Chemistry **146,** 13–21 (1999)
Article ID jssc.1998.8284, available online at http://www.idealibrary.com on IDEAL®

Surface Structure of Mechanically Activated and of Mechanosynthesized Zinc Ferrite

P. Druska[1] and U. Steinike

Institute of Applied Chemistry Berlin-Adlershof, 12484 Berlin, Germany

and

V. Šepelák[2]

Institute of Geotechnics of the Slovak Academy of Sciences, 043 53 Košice, Slovakia

Received January 20, 1998; in revised form March 12, 1999; accepted March 23, 1999

Zinc ferrite forms the structure of a normal spinel. A mechanical activation and a mechanosynthesis of zinc ferrite at room temperature lead to the formation of the metastable inverse spinel structure. The changes in the surface structure of mechanically activated and of mechanosynthesized zinc ferrite as a function of the mechanical treatment time and the relaxation of the mechanically induced inverse spinel structure by thermal treatment in the temperature range 800–1100 K have been studied using the ESCA method. The surface structure of the mechanically disturbed zinc ferrite, compared to the bulk structures of the inverse and normal spinels, and the mechanically induced increase in the reactivity are discussed. © 1999 Academic Press

Key Words: **ESCA; X-ray photoelectron spectroscopy; surface structure; mechanochemistry; mechanical activation; mechanosynthesis; spinel; zinc ferrite; surface structure; mechanically induced inversion; nanocrystalline material.**

1. INTRODUCTION

Zinc ferrite prepared by a conventional ceramic method forms the structure of a normal spinel with zinc in the tetrahedral [4] sites and iron in the octahedral [6] sites of a cubic close packing of oxygen atoms $Zn^{[4]}Fe_2^{[6]}O_4$ (1, 2). It is well known that the change in temperature may result in the change in the inversion degree of zinc ferrite, and that by rapid cooling from high temperature this spinel may be obtained in a "frozen in" inverse structure (3). A new mechanochemical method of zinc ferrite synthesis from a mixture of zinc oxide and iron oxide has received increased attention in recent years and offers the possibility of forming zinc ferrite inverse spinel structural state are shown in Fig. 1.

The structural disorder in the bulk of mechanosynthesized (synthesized by the high-energy milling of the ZnO/Fe_2O_3 mixture) and of mechanically activated (synthesized by the conventional thermal method, followed by mechanical treatment) zinc ferrite was studied in our previous work (6, 9, 10) using X-ray diffraction (XRD), Mössbauer spectroscopy, and electron microscopy. It was found that the metastable nanoscale structural state of both mechanically activated (mechanoactivated) and mechanosynthesized zinc ferrites is characterized by a substantial displacement of Fe^{3+} cations to tetrahedral sites and of Zn^{2+} cations into octahedral sites of the cubic close-packed anionic sublattice as well as by the deformation of the spinel octahedron geometry.

In situ X-ray powder diffraction proved satisfactory for quantitatively following the thermally induced structural evolution of mechanosynthesized and of mechanoactivated zinc ferrites during their thermal treatment in an XRK-A Paar camera (14, 15). The interval of the thermal stability of the mechanically induced defects in the structure of mechanosynthesized and of mechanoactivated zinc ferrite is up to 700 and 600 K, respectively (6, 14). The kinetic study of the thermally induced inverse–normal transition has revealed that the reequilibration in mechanosynthesized zinc ferrite proceeds rapidly in the temperature range 885–1073 K, and the activation energy of the transition is $E \sim 72\ \mathrm{kJ \cdot mol^{-1}}$ (15).

In recent years, zinc ferrite has been used as an absorbent material for hot-gas desulfurization (16, 17), capable of removing sulfur-containing species from coal gas. It is also capable of being regenerated for continuous use (18).

[1] To whom correspondence should be addressed at MTU Motoren- und Turbinen-Union, München GmbH, Dachauer Strasse 665, 80995 Munich, Germany.

[2] Current address: Humboldt Fellow at the Institute of Physical and Theoretical Chemistry, Technical University of Braunschweig, Pockelsstr. 14, 38106 Braunschweig, Germany.

0022-4596/99 $30.00

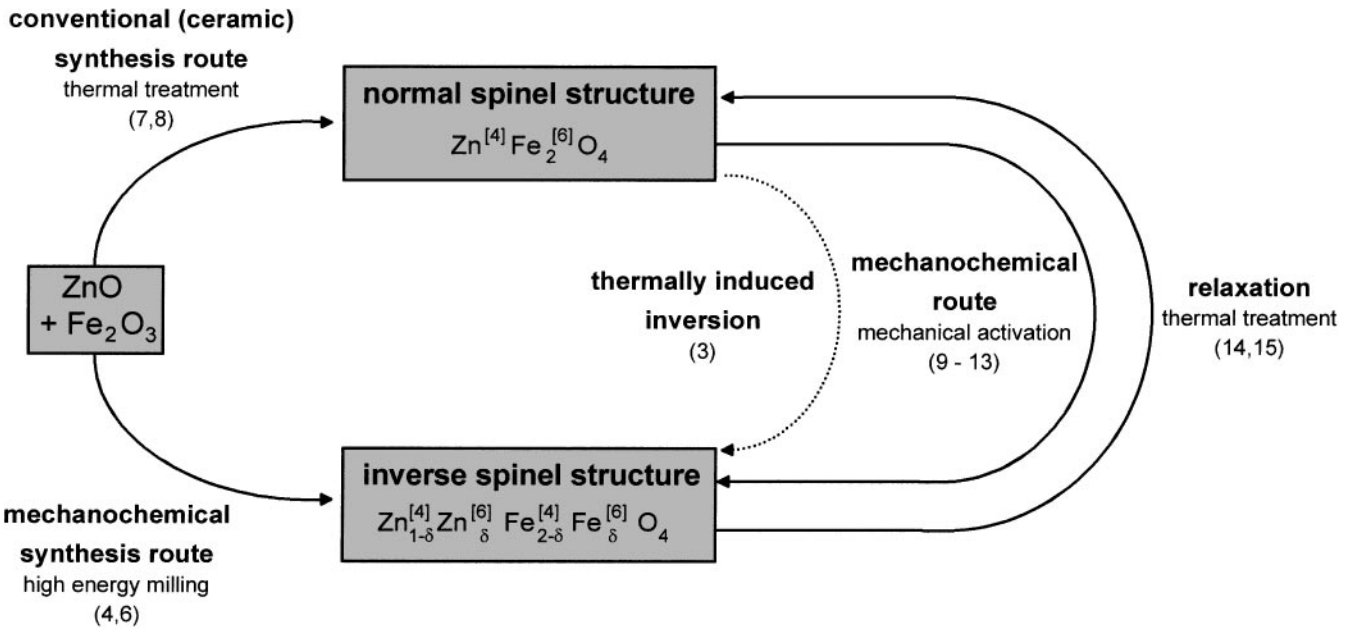

FIG. 1. Schematic circle of the conventional (ceramic) synthesis route and of the mechanochemical synthesis route of zinc ferrite, as well as of the formation of the metastable inverse spinel structure and of its relaxation (δ is the inversion degree).

High-temperature sulfurization tests of mechanosynthesized zinc ferrite with the components of coal gas have shown a striking increase in the sulfur absorption capacity compared with the reactivity of the unmilled α-Fe_2O_3/ZnO mixture as well as with the reactivity of mechanoactivated zinc ferrite (19, 20). Despite this favorable effect of the mechanochemical preparation route on the high-temperature reactivity of zinc ferrite, little is known of the surface structural state of this solid.

It is obvious that reactions of mechanosynthesized and of mechanoactivated zinc ferrite with components of coal gases in the desulfurization process are surface-sensitive and, at least, initiate on the surface of the mechanically treated spinels. It would be impossible to put forward interpretations of high-temperature sulfurization tests if the surface of these mechanically treated solid reactants were not well characterized.

Therefore, in the present work X-ray photoelectron spectroscopy (XPS), as a powerful surface analytical tool, was used to obtain information about the elemental composition of the outermost atom layers of mechanosynthesized and of mechanoactivated spinel, the chemical binding state, and the precise sites of the atoms in relation to the crystal structure of the mechanically disturbed surface.

2. EXPERIMENTAL

Two synthesis routes, a conventional thermal method and the mechanochemical route, were used for the preparation of zinc ferrite. Stoichiometric mixtures of powdered reactants containing 66.34% α-Fe_2O_3 and 33.76% ZnO by weight (products of Merck) were used as starting materials. The milling process was carried out in a planetary ball mill AGO 2 (Institute of Solid State Chemistry, Novosibirsk) at room temperature. Ten grams of the starting material was sealed in a stainless steel vial (150 cm^3 in volume) together with stainless steel balls of 5 mm in diameter. The ball-to-powder weight ratio was 20:1. Milling experiments were performed in air at 800 rpm.

The selected mechanically treated sample was heated isothermally: heating was carried out in an electric furnace, which was maintained at four selected temperatures for 4 h. At the completion of the heat treatment period the sample was removed from the furnace and cooled rapidly by air quenching. The investigated samples are summarized in Table 1.

The surface analytical studies were performed with an ESCALAB 220iXL spectrometer (Fisons Instruments) consisting of two vacuum chambers: the analyzer and the fast entry air lock/preparation chamber. The powdered samples were fixed on carbon-conductive tape (Pelco International) at the top of the sample holder and transferred into the ultrahigh vacuum. The X-ray source was monochromatic-focused A1$K\alpha$ radiation (1486.6 eV) with an input power of 150 W. The emerging charge of the sample was equalized with the installed charge compensation. The final peak position was determined using the C 1*s* peak (shifted to 285.0 eV) corresponding to absorbed carbon species. The XPS measurements were performed at a constant pass energy of 25 eV. The ESCALAB was calibrated routinely with

TABLE 1
List of the Samples Investigated

Sample No.	Compound	Time of mechanical treatment (min)	Temperature of isothermal treatment (K)
0	$ZnFe_2O_4$	0	—
I	$ZnFe_2O_4$	2	—
II	$ZnFe_2O_4$	18	—
III	$ZnO + Fe_2O_3$	0	—
IV[a]	$ZnO + Fe_2O_3$	8	—
V[b]	$ZnO + Fe_2O_3$	18	—
VI	$ZnO + Fe_2O_3$	18	800
VII	$ZnO + Fe_2O_3$	18	900
VIII	$ZnO + Fe_2O_3$	18	1000
IX	$ZnO + Fe_2O_3$	18	1100

[a] According to Šepelák *et al.* (6) this sample represents the partly mechanosynthesized zinc ferrite; ~ 30 wt% $ZnFe_2O_4$.

[b] According to Šepelák *et al.* (6) this sample represents almost completely mechanosynthesized spinel ferrite (ZnO/Fe_2O_3 mixture converted mechanochemically into a $ZnFe_2O_4$).

the appropriate XPS lines of Au, Ag, and Cu, as given in Ref. (21). The XPS spectra of the investigated samples were evaluated on the basis of well-characterized zinc standard compounds. After background correction according to Shirley (22), the zinc standard peaks were described with Gaussian–Lorentzian curves and with a tail function to take care of the asymmetry of the XPS signals (23).

The particle size distribution was measured by laser radiation scattering using the Laser-Particle-Sizer Analysette 22 granulometer (Fritsch, Idar-Oberstein). The mean particle diameter was estimated as the first moment of the volume size distribution function. The specific surface area was determined by the standard Brunauer–Emmett–Teller (BET) method using the Gemini 2360 apparatus (Sy-Lab, Vienna).

3. RESULTS AND DISCUSSION

Due to the facts that, in spinel ferrites, the oxygen anions always form a nearly close-packed cubic array, i.e., they have the same crystallographic positions in both normal and inverse spinel structures, and that the low-structured Fe $2p_{3/2}$ XPS signal corresponds to both octahedrally and tetrahedrally coordinated iron cations, the O 1*s* and the Fe $2p_{3/2}$ signals give no specific peak structures for a fundamental XPS analysis. Therefore, only the Zn $2p_{3/2}$ XPS signal was taken into account for the interpretation of the mechanically induced changes of the surface crystal structure of the investigated systems.

To obtain information about the elemental composition of the outermost atom layers, the chemical binding state, and the precise sites of atoms in relation to the surface crystal structure, we first analyzed in detail several coordinated zinc compounds, which served as reference model samples. The used standards were, on one hand, ZnO as a structurally well-known tetrahedrally coordinated species and, on the other hand, different zinc titanium oxides, described by Steinike and Wallis (24), such as, $Zn_2Ti_3O_8$ for the tetrahedrally coordinated zinc species and Zn_2TiO_4 and $ZnTiO_3$ for the octahedral coordination of zinc. Figure 2 shows the spectra of four standard substances, including the peak evaluation and the peak positions. The mathematic description of all zinc standard peaks gives a satisfactory solution with two Gaussian/Lorentzian peaks with tail parameters of every zinc species. These XPS peak parameters of the standards are listed in Table 2.

The data of Table 2 clarify that the XPS signals of the identically coordinated zinc compounds give roughly the same peak parameters. Therefore, for further XPS data evaluation the parameter sets of ZnO and Zn_2TiO_4 were used. On the basis of these standards, a quantitative evaluation of the XPS spectra of mechanoactivated and of mechanosynthesized zinc ferrite was performed. The information depth of the XPS measurements was given by the mean free path of the photoelectrons as described in (25). The mean free path of the photoelectrons in zinc oxides for the Zn $2p_{3/2}$ signal was estimated to be 1.961 nm, leading to the value of the information depth of ~ 6 nm (with the approximation that the information depth is three times that of the mean free path of photoelectrons).

Figures 3 and 4 summarize the behavior of the zinc ferrite and of the Fe_2O_3/ZnO mixture submitted to the high-energy milling process as a function of the milling time. The XPS measurements revealed that the Zn $2p_{3/2}$ signal of the starting ZnO/Fe_2O_3 mixture and of the nonactivated zinc ferrite consists of a single sharp peak corresponding to the tetrahedrally coordinated zinc. With increasing milling time, the Zn $2p_{3/2}$ signal in the spectra of both zinc ferrite and the oxide mixture becomes broader, and the second new component gradually appears on its right side. We notice that the new component of the signal is clearly visible in the XPS spectrum of mechanoactivated zinc ferrite already after 2 min of milling (Fig. 3). Further milling of the conventionally prepared zinc ferrite, as well as of the ZnO/Fe_2O_3 mixture, leading to a progressive mechanosynthesis of zinc ferrite (6), is accompanied by the gradual increase of the relative weight of the new signal component in the XPS spectra (Figs. 3 and 4).

Comparison of the XPS spectra for the mechanoactivated zinc ferrite and for the mechanosynthesized zinc ferrite revealed that, from the qualitative point of view, the surface structure of mechanosynthesized zinc ferrite is similar to that of the mechanically treated zinc ferrite. An interesting observation is that in the spectra of both mechanosynthesized and mechanoactivated zinc ferrites, the newly created component of the Zn $2p_{3/2}$ signal has the same peak

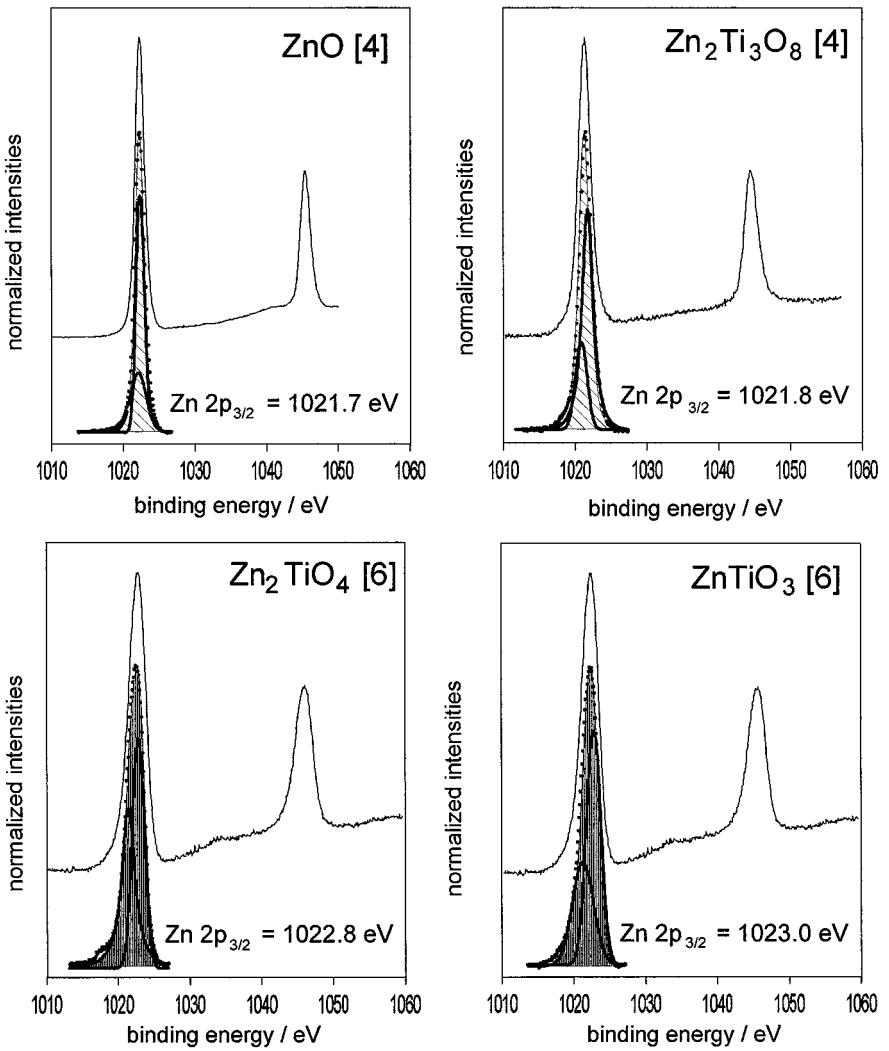

FIG. 2. Photoelectron spectra of Zn-model substances ZnO, Zn_2TiO_3, Zn_2TiO_4, and $ZnTiO_4$.

position as the signal assigned to the octahedrally coordinated zinc in Zn_2TiO_4 shown in Fig. 2. Thus, the Zn $2p_{3/2}$ signal corresponds not only to the tetrahedrally but also to the octahedrally coordinated zinc. Taking into account that zinc ferrite prepared by a conventional ceramic method adopts the normal spinel structure, in which divalent zinc cations occupy only sites tetrahedrally coordinated by oxygen while the octahedrally coordinated sites are occupied by the Fe^{3+} cations, an appearance of zinc in octahedral sites is evidence that, in addition to the bulk structure (6), the surface structure (<6 nm) of both mechanosynthesized and mechanoactivated zinc ferrites corresponds to the structure of the inverse spinel. In both cases, the fraction of Zn^{2+} ions in octahedral positions increases with increasing milling time. The exact parameters of the XPS data evaluation are given in Tables 3a and 3b.

The influence of mechanical treatment on the surface changes in solids has been assessed in a number of published papers in terms of changes in integral quantities such as particle size distribution, specific surface area, and mean particle size. Although at present these quantities are considered insufficient to describe the mechanically induced surface changes, they remain an important part of the complex description of a powdered system. In our case they complement the surface structure information obtained by XPS.

The sizes of the powder particles of the starting Fe_2O_3/ZnO mixture and of the nonactivated zinc ferrite varied from 10 to 20 μm, and the specific surface area was 4.8 and 4.1 $m^2\ g^{-1}$, respectively. In the course of milling, the powder particles were subjected to continuous fragmentation. As a result of mechanical activation, as well as of

TABLE 2
The XPS Peak Parameters of the Zn $2p_{3/2}$ Signals for Different Standard Compounds

	ZnO[a]	$Zn_2Ti_3O_8$	Zn_2TiO_4[a]	$ZnTiO_3$
Coordination number of zinc	[4]	[4]	[6]	[6]
Binding energy (eV)	1020.98	1021.02	1022.06	1022.03
	1021.68	1021.81	1022.82	1023.04
Relative height	0.248	0.361	0.693	0.535
	1.000	1.000	1.000	1.000
$\beta \approx$ FHWM	1.245	1.203	1.583	1.665
	0.843	0.948	1.275	1.368
G/L	0.020	0.092	0.975	0.943
	0.000	0.000	0.000	0.025
TM	0.280	0.275	0.000	0.007
	0.000	0.000	0.000	0.008
CT	0.003	0.008	0.012	0.019
	0.005	0.014	0.024	0.022
ET	0.485	0.394	0.335	0.256
	0.157	0.119	0.255	0.202

Note. (G/L is the Gaussian/Lorentzian ratio, TM is the tail mixing ratio, CT is the constant tail ratio, and ET is the exponential tail ratio.

[a] This parameter set is used for the XPS data evaluation of both mechanoactivated and mechanosynthesized zinc ferrites.

mechanochemical reaction, the powders become much finer and uniform in shape. While the starting powders consisted predominantly of individual particles, the samples of both mechanoactivated and mechanosynthesized zinc ferrites consisted of aggregates of fine particles. Aggregation was observed by electron microscopy in our previous work (6, 14, 19). Stable aggregates behave under the condition of particle size analysis as individual particles and thus the "real" mean particle diameters of both mechanoactivated and mechanosynthesized zinc ferrites are smaller than the determined value, $d_m \sim 1$ μm. The specific surface areas of the starting powders and of the powders obtained are compared in Fig. 5.

The new surface formation, alteration in the geometry of isolated particles and secondary aggregates, and changes in the energetic state of the structure in the near-surface layers, caused by the high-energy milling, are accompanied by structural disorder in the bulk of mechanoactivated and mechanosynthesized zinc ferrite. Results of the X-ray diffraction study of the structure of mechanoactivated zinc ferrite, reported in our previous work (9, 10, 14), revealed that the inversion degree δ, defined as the fraction of octahedral sites occupied by Zn^{2+} cations, monotonically increases with increasing milling time from 0 to 0.94; i.e., the normal spinel is, after a relative short time of milling (24 min), almost completely converted into the inverse one (Fig. 6). In contrast to the XRD measurements, the XPS investigations have revealed that only a part of the surface structure of mechanoactivated (69%) and of mechanosynthesized (35%) zinc ferrite is transformed into the inverse spinel structure.

Variation of the inversion degree of both mechanoactivated and mechanosynthesized zinc ferrites with the milling time is shown in Fig. 6. It should be emphasized that while the inversion degree estimated by the XRD reflects the total structural disorder in the bulk, lower values of the

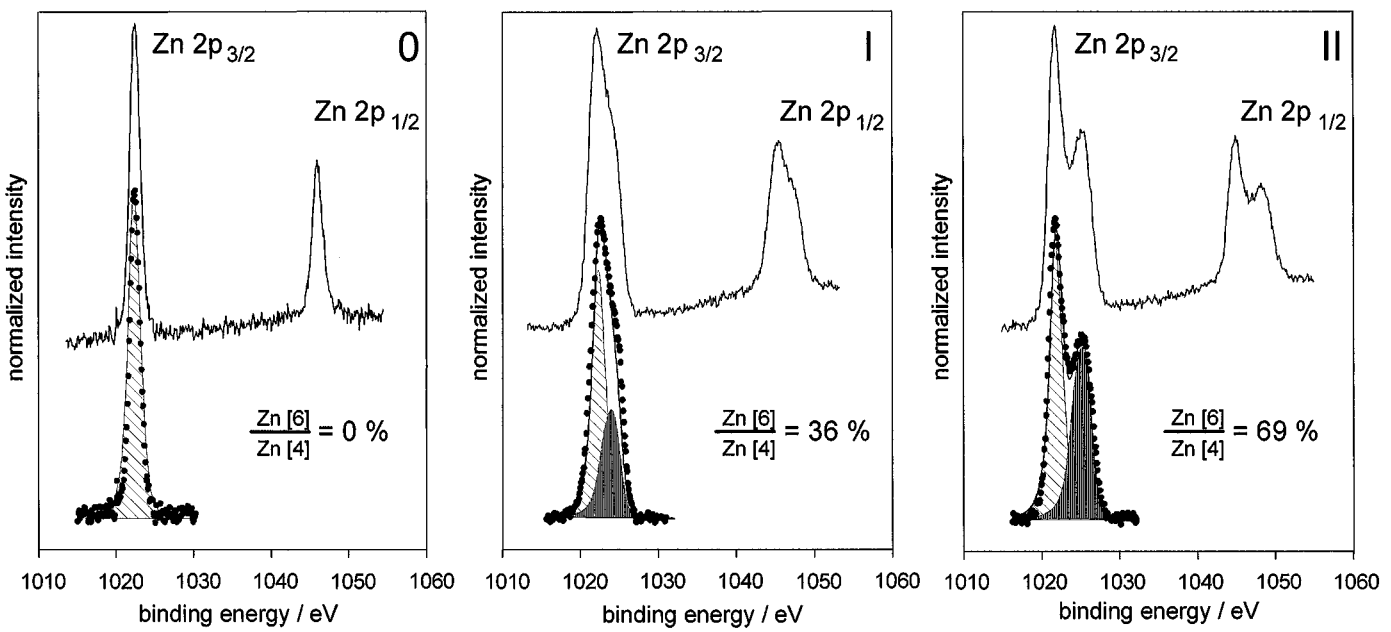

FIG. 3. Photoelectron spectra of zinc ferrite: (0) $ZnFe_2O_4$ (nonactivated material); (I) $ZnFe_2O_4$ mechanoactivated for 2 min; (II) $ZnFe_2O_4$ mechanoactivated for 18 min.

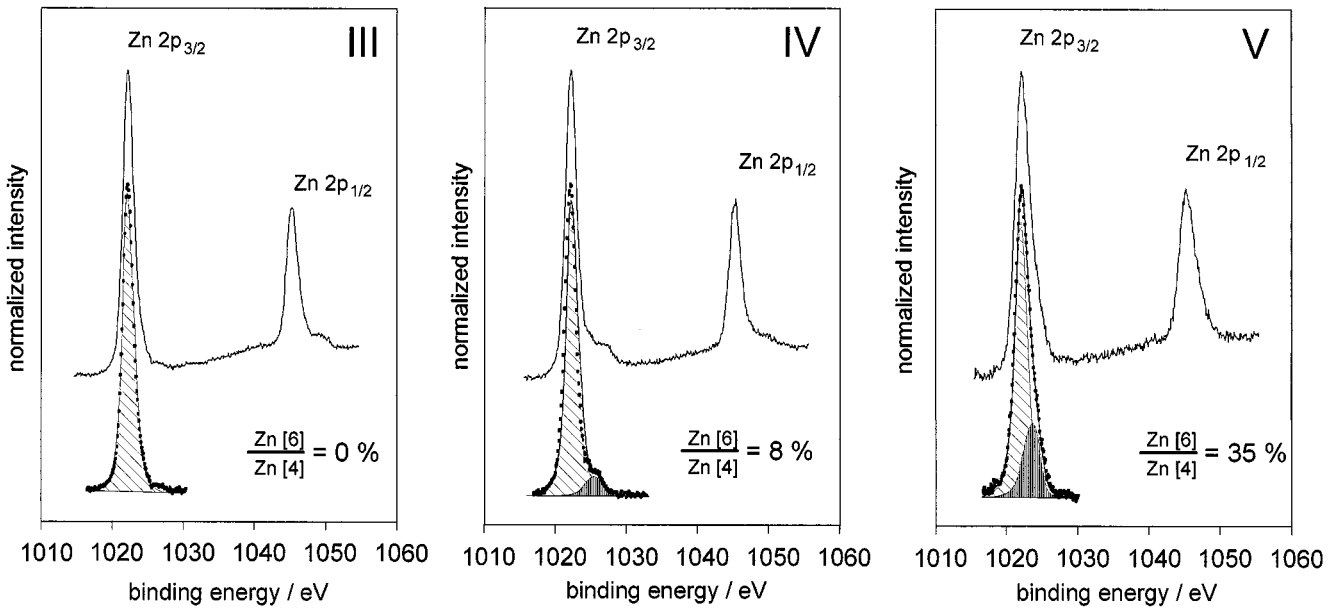

FIG. 4. Photoelectron spectra of the Fe_2O_3/ZnO mixture: (III) the Fe_2O_3/ZnO mixture (unmilled); (IV) the Fe_2O_3/ZnO mixture milled for 8 min (after (6), this sample represents the partly mechanosynthesized zinc ferrite; $\sim$30 wt% $ZnFe_2O_4$); (V) the Fe_2O_3/ZnO mixture milled for 18 min (after (6), this sample represents almost completely mechanosynthesized zinc ferrite).

inversion degree of the surface structure ($0 < \delta < 0.69$), determined by XPS, are probably caused by the low information depth of the ESCA method as well as by a recombination of the surface cations (e.g., with ions from the atmosphere) whose bonds become broken and unsaturated during the mechanical treatment. The surface of the milled material is so reactive that the structural reorganization of the disturbed surface takes place quickly by catalysis of the atmosphere. Thus, evaluation of the inversion degree using the XRD method leads to higher values than those estimated by the XPS method, i.e.,

$$\delta_{\text{bulk}} > \delta_{\text{surface}}.$$

The difference between δ_{bulk} and δ_{surface} is more significant in mechanosynthesized zinc ferrite than in mechanoactivated spinel (Fig. 6). Mechanically induced redistribution of the surface cations indicates that the mechanically treated samples exhibit a highly disturbed surface structure with a number of broken and unsaturated bonds. Differential thermal analysis (DTA) and thermogravimetry (TG) investigations of both mechanoactivated and mechanosynthesized zinc ferrites have revealed that the amount of adsorbed atmospheric gases on the mechanically disturbed surface increases with increasing surface area of the systems investigated (15). Taking into account the larger specific surface area of mechanosynthesized zinc ferrite

TABLE 3a
XPS Spectrum Parameters of the Nonactivated Zinc Ferrite and of Mechanoactivated Zinc Ferrite for Various Milling Times

	Sample 0	Sample I	Sample II
Zn in tetrahedral coordination			
Concentration (at.%)	100	73.49	59.22
Binding energy (eV)	1021.80	1021.67	1021.62
Zn in octahedral coordination			
Concentration (at.%)	0	26.51	40.78
Binding energy (eV)	—	1023.20	1023.27

TABLE 3b
XPS Spectrum Parameters of the Starting ZnO/Fe_2O_3 Mixture and of Mechanosynthesized Zinc Ferrite from Zinc Oxide and Hematite as a function of the Milling Time

	Sample III	Sample IV	Sample V
Zn in tetrahedral coordination			
Concentration (at.%)	100	92.47	74.03
Binding energy (eV)	1022.05	1021.98	1021.87
Zn in octahedral coordination			
Concentration (at.%)	0	7.53	25.97
Binding energy (eV)	—	1023.21	1022.94

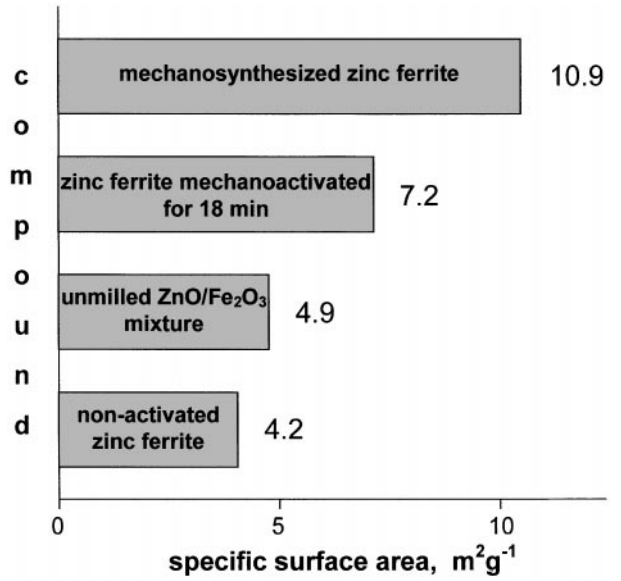

FIG. 5. Specific surface area of the starting compounds and of the mechanically treated powders.

(10.9 $m^2\ g^{-1}$) in comparison with the mechanoactivated zinc ferrite (7.2 $m^2\ g^{-1}$), it may be assumed that the number of recombined surface cations (respectively, saturation of their bonds with ions from the atmosphere) in mechanosynthesized zinc ferrite is higher than that in the case of the mechanically activated spinel. In addition to this assumption, the difference in inversion degree of the surface structure between mechanosynthesized and mechanoactivated samples may be attributed to the incomplete mechanochemical conversion at early stages of the mechanical treatment.

A further aspect, which was studied only to a limited extent until now, is related to the thermal stability of mechanically induced structural defects in these solids and the mechanism of their relaxation at heating. Since in the process of relaxation of mechanically induced metastable states the advantageous properties of mechanically treated solids are mostly lost, it is necessary to know the lifetime of the activated surface and the time dependence of the relaxation. This understanding would be of principal importance from the scientific point of view in the development of an atomistic and microscopic theory of the mechanochemical processes, as well as from the practical point of view in the application of mechanically treated solids at elevated temperatures.

The XPS spectra of mechanosynthesized zinc ferrite after the thermal treatment at various temperatures are shown in Fig. 7. The corresponding XPS data, given in Table 4, indicate that the relaxation of the surface structure starts at $T > 800\,K$ and is complete at temperatures above 1000 K within a period of 4 h. Thus, the metastability of the surface structure of mechanosynthesized zinc ferrite at heating is manifested in the gradual disappearance of the mechanically induced inversion. The reequilibration of the surface structure terminates by a complete relaxation; i.e., the surface structure of mechanosynthesized spinel is transformed into a normal spinel structure upon heating (typical of the crystalline zinc ferrite prepared by the conventional thermal method). These results correspond to the information on the

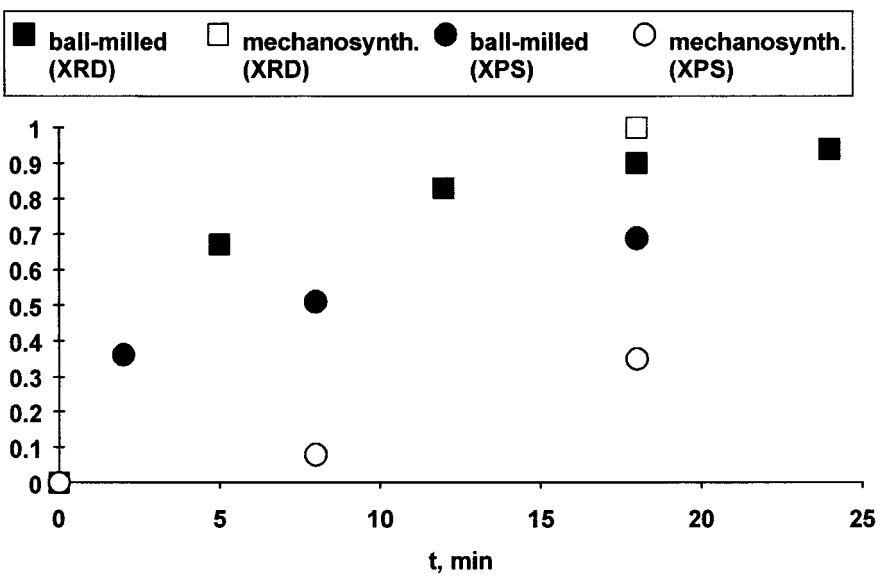

FIG. 6. Dependence of the inversion degree (δ) of the mechanoactivated zinc ferrite (full points) and of the mechanosynthesized zinc ferrite (empty points) on the time of mechanical treatment (t). The experimental method which was used for determination of the inversion degree is indicated in parentheses.

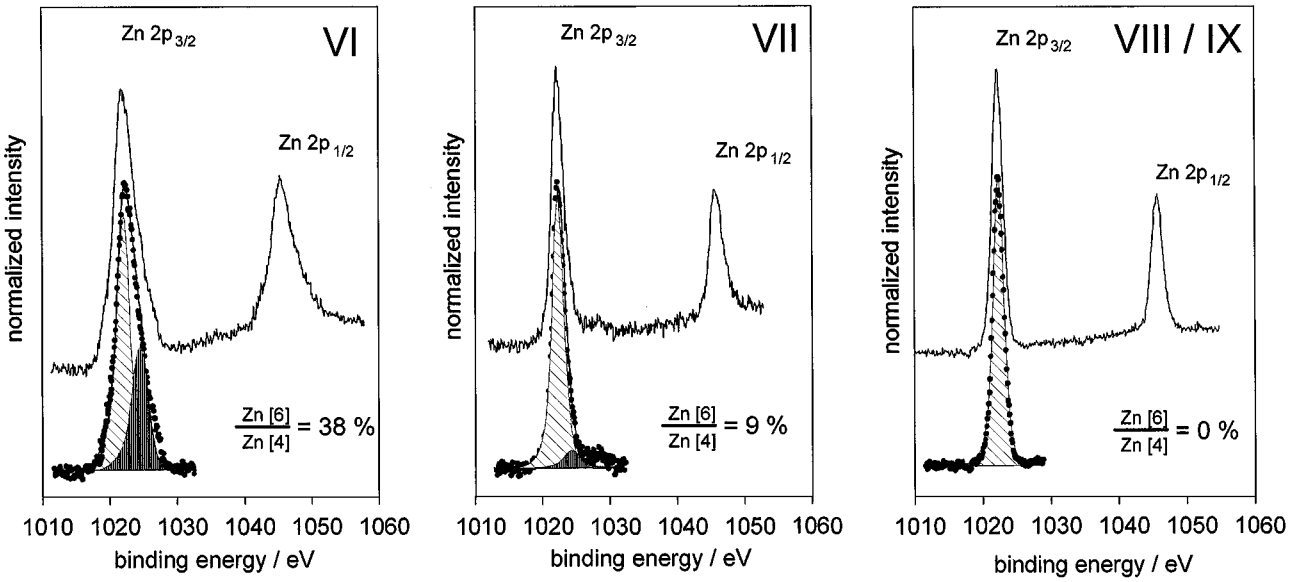

FIG. 7. Photoelectron spectra of mechanosynthesized zinc ferrite taken after the thermal treatment at 800 K (VI), 900 K (VII), 1000 K (VIII), and 1100 K (IX).

bulk structure reequilibration, obtained by *in situ* X-ray diffraction, TG, and DTA, which will be reported in our further work (15).

The information on the surface structure and its response to changes in temperature, presented above, is very helpful in the interpretation of the results of the high-temperature sulfurization tests of mechanoactivated and mechanosynthesized zinc ferrite, reported in our previous work (19, 20).

It should be emphasized that the high-temperature sulfurization tests were carried out at 670 K (19) and 820 K (20), i.e., at temperatures at which the mechanoactivated and mechanosynthesized zinc ferrite absorbents are characterized by a high degree of dispersity and by the nanoscale nature of their structure (6, 26). However, the results presented in this paper have revealed that the presence of a fraction of cations in metastable inversion sites may be considered a main source of the structural metastability of the surface of mechanically treated absorbents. The increased mobility of cations at the sulfurization temperature, connected with their thermally stimulated return from the inversion into equilibrium sites, is evidently the main reason for an increased absorption capacity of the mechanically treated zinc ferrites. Moreover, the high-temperature sulfurization process is favorably influenced also by the size of the powder particles and surface area of the sorbent.

TABLE 4
Fitting Data of the XPS Spectra of Thermally Treated Mechanosynthesized Zinc Ferrite

	Sample VI	Sample VII	Sample VIII	Sample IX
Zn in tetrahedral coordination				
Concentration (at.%)	72.44	91.48	100	100
Binding energy (eV)	1021.07	1021.87	1022.18	1021.96
Zn in octahedral coordination				
Concentration (at.%)	27.56	8.52	0	0
Binding energy (eV)	1023.46	1023.27	—	—

4. CONCLUSIONS

The quantitative analysis of the XPS data evaluated on the basis of well-characterized zinc standard compounds yields detailed information about the surface structure of mechanoactivated and mechanosynthesized zinc ferrite. The results obtained in this work indicate that, from the qualitative point of view, the surface structure of the nanoscale mechanosynthesized zinc ferrite is similar to that of the mechanoactivated zinc ferrite (synthesized by the conventional ceramic method, followed by mechanical treatment). The main feature of the surface structural disorder of both mechanoactivated and mechanosynthesized zinc ferrites is the mechanically induced inversion. In both cases, the inversion degree increases with increasing milling time. At temperatures over 800 K the structural metastability of the surface of mechanosynthesized zinc ferrite is manifested in a gradual disappearance of the mechanically induced inversion. The reequilibration results in a complete relaxation of

the disordered surface structure. The mechanically induced reactivity of zinc ferrite is the result of its high degree of dispersity as well as of its structural metastability, which is connected with the mechanically induced disorder and with the nanoscale nature of its structure.

ACKNOWLEDGMENTS

This work was supported by the German Federal Ministry of Education, Science, Research and Technology and the Berlin Senate Department for Science, Research and Culture (Project 03C3005). The authors are indebted to the Deutsche Forschungsgemeinschaft (Projects Ste 692/2-1) and to the Alexander von Humboldt Foundation for financial support of one of them (V. Šepelák) during his stays at the Institute of Applied Chemistry in Berlin-Adlershof.

REFERENCES

1. R. J. Hill, J. R. Craig, and G. V. Gibs, *Phys. Chem. Minerals* **4,** 317 (1979).
2. C. P. Marshall and W. A. Dollase, *Amer. Mineral.* **69,** 928 (1984).
3 .H. St. C. O'Neill, *Eur. J. Mineral.* **4,** 571 (1992).
4. V. Šepelák, A. Yu. Rogachev, U. Steinike, D.-Chr. Uecker, F. Krumeich, S. Wißmann, and K. D. Becker, *Mater. Sci. Forum* **235–238,** 139 (1997).
5. V. Šepelák, A. Yu, Rogachev, U. Steinike, D.-Chr. Uecker, S. Wißmann, and K. D. Becker, *Acta Crystallogr. Suppl. Issue A* **52,** C-367 (1996).
6. V. Šepelák, U. Steinike, D.-Chr. Uecker, S. Wißmann, and K. D. Becker, *J. Solid State Chem. J. Solid State Chem.* **135,** 52 (1998).
7. I. Halikia and E. Milona, *Can. Metall. Quart.* **33,** 99 (1994).
8. H. Schmalzried, "Solid State Reactions." Verlag Chemie, Weinheim, 1981.
9. V. Šepelák, K. Tkácová, V. V. Boldyrev, S. Wißmann, and K. D. Becker, *Physica B* **234–236,** 617 (1997).
10. V. Šepelák, K. Tkácová, V. V. Boldyrev, and U. Steinike, *Mater. Sci. Forum* **228–231,** 783 (1996).
11. Yu, T. Pavlyukhin, Ya. Ya. Medikov, and V. V. Boldyrev, *J. Solid State Chem.* **53,** 155 (1984).
12. A. E. Ermakov, E. E. Yurchikov, E. P. Elsukov, V. A. Barinov, and Yu. T. Chukalkin, *Fiz. Tverd. Tela* **24,** 1947 (1982).
13. A. I. Rykov, Yu. T. Pavlyukhin, and Ya. Ya. Medikov, *Proc. Indian Natl. Sci. Acad., Part A* **55,** 721 (1989).
14. K. Tkácová, V. Šepelák, N. Števulová, and V. V. Boldyrev, *J. Solid State Chem.* **123,** 100 (1996).
15. V. Šepelák, U. Steinike, D.-Chr. Uecker, and D. Schultze, unpublished results.
16. R. E. Ayala and D. W. Marsh, *Ind. Eng. Chem. Res.* **30,** 55 (1991).
17. L. A. Bissett and L. D. Strickland, *Ind. Eng. Chem. Res.* **30,** 170 (1991).
18. A. Silaban, D. P. Harrison, M. H. Berggren, and M. C. Jha, *Chem. Eng. Comm.* **107,** 55 (1991).
19. V. Šepelák, U. Steinike, D.-Chr. Uecker, R. Trettin, S. Wißmann, and K. D. Becker, *Solid State Ionics* **101–103,** 1343 (1997).
20. V. Šepelák, K. Jancke, J. Richter-Mendau, U. Steinike, D-Chr. Uecker, and A. Yu. Rogachev, *Kona* **12,** 87 (1994).
21. M. T. Anthony and M. P. Seah, *Surf. Interface Anal.* **6,** 95 (1984).
22. D. A. Shirley, *Phys. Rev. B* **5,** 4709 (1972).
23. R. O. Ansell, T. Dickinson, A. F. Povey, and P. A. M. Sherwood, *J. Electroanal. Chem.* **98,** 79 (1979).
24. U. Steinike and B. Wallis, *Cryst. Res. Technol.* **32,** 187 (1997).
25. M. P. Seah and W. A. Dench, *Surf. Interface Anal.* **1,** 2 (1979).
26. V. Šepelák, M. Zatroch, K. Tkácová, P. Petrovic, S. Wißmann, and K. D. Becker, *Mater. Sci. Eng. A, Rapidly Quenched and Metastable Materials Supplement*, 22 (1997).